Available online at www.sciencedirect.com

jmr&t Journal of Materials Research and Technology

journal homepage: www.elsevier.com/locate/jmrt

Original Article

Ultra-permeable CNTs/PES membranes with a very low CNTs content and high H2/N2 and CH4/N2 selectivity for clean energy extraction applications

Samy Yousef [a,d,*], *Simona Tuckute* [b], *Andrius Tonkonogovas* [c], *Arūnas Stankevičius* [c], *Alaa Mohamed* [e]

[a] *Department of Production Engineering, Faculty of Mechanical Engineering and Design, Kaunas University of Technology, LT-51424, Kaunas, Lithuania*

[b] *Center for Hydrogen Energy Technologies, Lithuanian Energy Institute, Breslaujos 3, 44403, Kaunas, Lithuania*

[c] *Lithuanian Energy Institute, Laboratory of Heat Equipment Research and Testing, Breslaujos 3, LT 44403, Kaunas, Lithuania*

[d] *Department of Materials Science, South Ural State University, Lenin Prospect 76, 454080, Chelyabinsk, Russia*

[e] *Department of Production Engineering and Printing Technology, Akhbar Elyom Academy 6th of October, Egypt*

ARTICLE INFO

Article history:
Received 2 May 2021
Accepted 27 October 2021
Available online 30 October 2021

Keywords:
Polysulfone membranes
CNTs/PES membranes
Gas separation
H2/N2 selectivity
CH4/N2 selectivity
Clean energy

ABSTRACT

Polysulfone (PES) membranes are among the rare membranes that are capable of double filtration: a pre-filter layer captures agglomerates and a thin-dense layer is responsible for the main separation process. This work aims to enhance the permeability and H_2/N_2 and CH_4/N_2 of the dense layer of PES by mixing it with low concentrations of carbon nanotubes (CNTs: 0.01–0.03 wt.%) using solution casting and doctor blade techniques. The pore topology, microstructure, chemical, thermal, and mechanical properties of the synthesized CNTs/PES membranes were investigated using FTIR, XRD, TGA, and a universal testing machine, while permeability of single CO_2, H_2, N_2, and CH_4 permeability of the CNTs/PES membranes were tested under different temperatures (20–60 °C) and pressures (1–6 bar). Also, the effect of added CNTs, separation temperature, and pressure on the gas separation mechanism were investigated. The results showed that adding of CNTs contributed to increase in porosity from 81.7% (PES) to 88.4% (CNTs/PES) and decrease in pore sizes from 84 nm (PES) to 50 nm (CNT_S/PES). Meanwhile, the thermal and mechanical analysis showed that CNTs/PES membranes had higher thermal stability and somewhat lower strength compared with neat membranes. Also, the permeability measurements showed a big increase when only 0.01 wt.% of CNTs had been added, where H_2, CH_4, N_2, CO_2 permeabilities were increased up to 28,553, 11,358, 7540, 6720 Barrer, respectively, vs 10.4, 4.6, 13.7, and 12.3 Barrer in case of PES membranes. In addition, CO_2/N_2, CH_4/N_2, and H_2/N_2 selectivity of CNTs/PES membranes were enhanced by 29%, 396%, and 426%, respectively, as a result of pores refining and increasing of free space in the prepared CNTs/PES membranes. According to these results, CNTs/PES membranes with small loading of CNTs have a

* Corresponding author.
E-mail address: ahmed.saed@ktu.lt (S. Yousef).

https://doi.org/10.1016/j.jmrt.2021.10.125

tremendous ability to deal with separation of H_2/N_2 and CH_4/N_2, what make them promising candidates for clean energy extraction applications.

1. Introduction

Recently, the demand and investments in the production of polymer membranes have increased significantly and this method has been adapted as an emerging technology in many fields, including water treatment, oil separation, energy, protein extraction, etc. Because of unique porous structure of polymer membranes, ease of operation and installation, cheapness, and big separation efficiency, when compared to other methods (e.g., amino technology) [1–3]. All these advantages served as a strong motivation to employ polymer membranes technology in gas separation that was facing the terrible increment in environmental challenges, including carbon emissions [4,5]. Also, due to high permeability and selectivity, it has been used in biogas purification and upgrading [6]. Despite the tremendous success of membranes in gas separation and biogas upgrading at the laboratory level, the membrane fouling represents one of the major challenges, which appears when the method is applied at industrial scale, because feeding gas usually contains large particles and agglomerates leading to clogging of the porous structure of membranes, reduction of the method's efficiency and lifetime [7,8].

In order to address these limitations, the membranes with double filtration stages were developed. These types of membranes are composed of two layers: thick and dense layers. The thick layer has bigger pores in the range of 5–20 μm and acts as a pre-filter stage to capture large agglomerates and particles [9]. Also, this layer plays an important role in preventing the passage of large particles, which can help to prevent clogging of the porous structure of the membranes. Meanwhile, the thin-dense layer used as an ultrafiltration stage can be used for gas separation with smaller particles [10]. Polysulfone (PES) membrane is one of these membranes that have the property of double filtration and it has been recently used in gas separation with high selectivity [11,12]. Based on the pore size of PES membrane, Knudsen diffusion approach is applied for the gas separation mechanism, assuming that the gas separation is possible because molecules frequently collide with the pore wall [13,14]. Also, Kamble et al. (2020) measured the CO2/N2 and CO2/CH4 selectivity of PES membranes at room temperature and low pressure (0.5–1.5 bar) for potential applications in biogas upgrading [15], where biogas was usually composed of numerous gases (e.g., CO2, N2, etc.) mixed with the flammable gases (H2 and CH4), thus affecting negatively the performance and economic value of this energy product and the separation process [16,17]. The agglomerates, nitrogen and carbon are considered to be the main contamination sources in biogas and these particles tend to clump together as a result of the force of attraction between particles gases, what leads to formulation of many agglomerates particles and causes serious piping problems, such as corrosion [18–20].

Therefore, PES nanocomposite membranes were introduced to overcome these problems. In case of such membranes, the main substance was mixed with different types of inorganic fillers to overcome the above-mentioned limitations to a large extent. In addition, the chemical, thermal, permeability, selectivity performance of the PES nanocomposite membranes were improved. Also, these fillers can reduce membrane fouling, as well. In the literature, there are various types of filler materials used for that purpose, such as SiO2, ZnO, Ag, graphene nanoparticles, carbon nano-fibre (CNF), carbon nanotubes (CNTs), etc. [9,21–24]. Among all these fillers, CNTs demonstrated a distinctive performance in gas separation, water treatment, oil–water mixture separation, etc. It was achieved because of their unique structure, as they consist of hollow tubes with an inner diameter lower than <100 nm that allow passage of smaller particles within ultrafiltration or nanofiltration scope [25–28]. Also, it was manifested that addition of CNTs was sufficient to cause fundamental changes in the membrane morphology and that CNTs are promising materials as absorbents or inorganic fillers for membranes. Also, the incorporation of CNTs to PES membranes could have caused fundamental changes in the membrane morphology. In addition, CNTs are promising materials as absorbents with good chemical, thermal, and mechanical properties that can be used to enhance the main physical and chemical properties of the membranes [29–32].

In the literature, several old studies, how CNTs improve the selectivity and permeability of PES membranes were found. The experiments were performed by loading CNTs in the range of 0.5–10 wt.% [33,34]. Also, these studies were focused on studying CO_2/N_2 and $CO2/CH_4$ selectivity and the results showed that the highest $CO2/N_2$ and $CO2/CH_4$ selectivity can be achieved at 5 wt.% and 0.5 wt.% of CNTs, respectively. Although the results showed that the separation process became more efficient, but still these results are are doubtful, especially as the modern studies showed that at lower concentrations of CNTs (<0.1 wt.%), a uniform dispersion can be achieved, avoiding any agglomeration, thus improving permeability of the membranes [35,36], while at higher percentage, CNTs started to agglomerate, thus clogging the pores of membranes and eliminating the high area-to-volume ratio characteristics and obstructing the gas transportation through the synthesized membranes, leading to decrease in the lifetime of membranes and high operating costs [37]. Also, the selectivity was measured at room temperature and at constant pressure (3 and 4 bars) without paying any attention to their impact on performance. Within this context, this research aims to enhance the permeability of PES by mixing it with a small amount of CNTs (0.01, 0.02, and 0.03 wt.%) and

investigates their potential applications in gas separation and carbon capture. Also, the possibility of using the prepared membranes in H2 and CH4 separation was studied with regard to the unconventional natural gas upgrading systems, especially when these gases were characterised as having a high energy transferring efficiency with smaller emission and being cheaper [38,39]. The experiments in the present work started with the preparation of CNTs/PES films with different concentrations of CNTs using a solution casting route and a doctor blade approach. Subsequently, the physical, chemical, morphological, thermal, and mechanical properties of the synthesized membranes were analysed. After that, H2, CH4, N2, CO2 permeabilities of the prepared membranes were measured at 20–60 °C and 1–6 bar. Finally, CO2/N2, CO2/H2, CO2/CH4, CH4/N2, and H2/N2 selectivity of CNTs/PES membranes was estimated.

2. Experimental

2.1. Materials

Polyethersulfone pellets (PES: with molecular weight of 75,000 g mol^{-1}), Polyvinylpyrrolidone (PVP), Dimethylformamide (DMF), and other reagents (sulfuric acid (H2SO4), nitric acid (HNO3), etc.) were supplied by Sigma–Aldrich. Carbon nanotubes (CNTs) with average diameter of 25 were synthesized using a CVD device [40]. Then they were exposed to chemical functionalization process in order to remove the impurities and amorphous carbon, and to modify the surface of the synthesized CNTs. The functionalization process started with oxidizing CNTs at 170 °C in a mixture of H2SO4 and HNO3 (w/w 3:1) for 60 min, then washing the filtrated powder and drying at 60 °C for overnight [41]. Finally, CO2, N2, H2, and CH4 gases with purity ≥99.99% were supplied by the Lithuanian Energy Institute, Lithuania.

2.2. Design of the research experiments

The experiments in the current work were developed in four phases: a) preparation of the PES nanocomposite membranes with different concentrations of CNTs (0.01 wt.% "CNTs/PES1", 0.02 wt.% "CNTs/PES2", and 0.03 wt.% "CNTs/PES3"), b) physical, chemical, microstructural, thermal, and mechanical characterizations of the fabricated membranes, c) gas separation measurements, and d) gas separation mechanism. All these phases, including their optimum conditions, are explained in detail in the following sections.

2.3. Fabrication of PES nanocomposite membranes

Fig. 1 shows the preparation stages of CNTs/PES membranes used in the present research. As shown in the layout, the phase-inversion technique was used to fabricate PES membranes and their nanocomposite with different concentrations of CNTs (0.01, 0.02, and 0.03 wt.%). The fabrication process started with the preparation of PES solution by mixing 14 wt.% of PES pellets and 1 wt.% of PVP in DMF solvent. Afterwards, CNTs were added to the mixture and mixed together using a magnetic stirrer at 50 °C for 6 h, then mixed again for 1 h under the effect of soundwave at 50 °C, thus preparing the CNTs/PES solutions with a uniform distribution (Fig. (1A)). In order to prepare the CNTs/PES membranes with a uniform thickness (~100 μm), ZAA 2300-automatic film applicator with a casting knife was employed to cast the doping solution on a glass substrate at 20 mm/s (Fig. (1B)). Then the glass plate with CNTs/PES film was subsequently immersed into DI water in a coagulation bath for 15 min at 75 °C for drying process (Fig. (1C)); then the CNTs/PES films were peeled off the glass substrate and dried again in a vacuum oven at 27 °C for overnight. In order to remove the residual solvent, the dried films were kept in pure water all day long, thus preparing the final CNTs/PES membranes with surface area of 220 mm × 170 mm, as shown in Fig. (1D). Finally, the mechanical samples (length of 100 mm and width of 10 mm) were cut from the prepared sheets using a shaper cutter for mechanical measurements. Also, round shapes with diameter of 60 mm were cut from sheets for gas permeability measurement, as shown in Fig. (2).

2.4. Membrane characterizations

The scanning electron microscope (SEM) was used to examine the dispersion of CNTs in the prepared membranes. Also, surface and cross-section morphology of CNTs/PES membranes was observed using SEM. The capillary flow porometer (Porometer 3G zh, Quantachrome, Anton Paar GmbH, Germany) was used to determine the pore sizes of the prepared membranes and to check their integrity in the liquid solution followed by drying on the holder [42]. The porosity of CNTs/PES membranes and their pore size were measured by using mercury intrusion porosimetry (MIP, Pascal 440 Evo, Thermo Scientific) based on the following conditions: Pressure (400 MPa), temperature (21 °C), mercury density (13,439 g/cm^3), and filling volume (450 mm^3). The chemical structure of CNTs/PES membranes and their functional groups was analysed using the X-ray crystallography (XRD) and Fourier-Transform

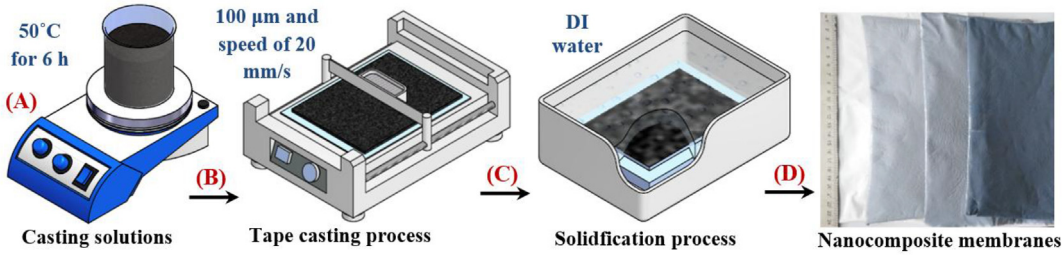

Fig. 1 – Preparation stages of CNTs/PES membranes.

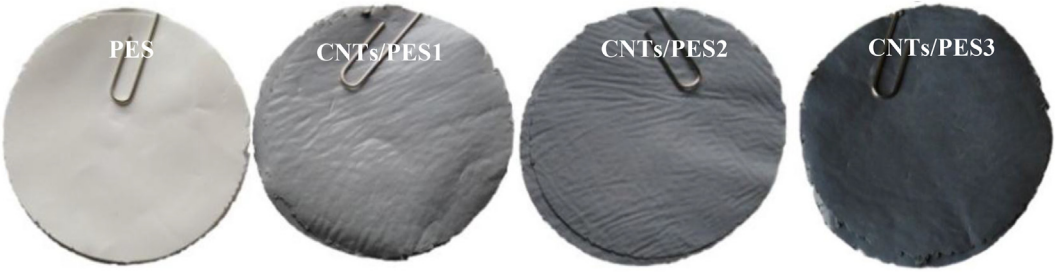

Fig. 2 – Images of the synthesized CNTs/PES membranes.

Infrared spectroscopy (FTIR). Meanwhile, the mechanical properties of the prepared CNTs/PES membranes were measured using the Lloyd Universal Testing Machine (model LR10K) at 5 mm/min. In addition, the thermal decomposition of the synthesized CNTs/PES membranes was analysed in nitrogen atmosphere at 20 °C/min using Thermogravimetric analysis (TGA-DTG) up to 900 °C.

2.5. *Gas permeation measurements*

The gases (CO2, H2, N2, and CH4) permeation measurements were carried out at different temperatures (20, 40, and 60 °C) and different absolute pressures in the range of 1–6 bars using the permeation apparatus shown in Fig. (3A). It is clear that the apparatus contained sources of gases, a membrane permeation module, and a gas measurement system. As shown in the figure, the setup consisted of different sources of gases (CO2, H2, N2, and CH4) to be able to control their flow rate and pressure using regulators/transducer. The membrane permeation module in the form of circular block was composed of two flanges, a tight sealing system with rubber O-rings, and a porous thin metal disc with total porous area of 2.88 cm^2 (used as a support wall for the tested CNTS/PES membranes). In order to measure the permeability of the selected gases, the round CNTs/PES membrane was tightly enclosed into the membrane permeation module, the membranes were held in vacuum for approximately 3 min to reach a steady state, and then exposed to selected gas at a specific temperature and pressure.

Finally, the volumetric flow rate measurements of permeated gases (CO2, H2, N2, and CH4) were collected using a soap bubble flowmeter. Finally, the gas permeability ($P_{i,j}$) and selectivity were determined by Eq. (1) and (2); all parameters are defined in Table 1 [43]. In order to improve the results' accuracy, the gas experiments of each gas were performed three times and the average measurements were recorded.

$$P_{i,j}(\text{Barrer}) = \frac{\frac{Q_{i,j}}{A}\left(\frac{cm^3}{s.\ cm^2}\right) x\ l\ (cm)}{\Delta P\ (cmHg)} \quad (1)$$

$$\alpha_{i/j} = \frac{P_i}{P_j} \quad (2)$$

3. Results and discussion

3.1. *Morphology of the synthesized CNTs/PES membranes*

In order to prepare the SEM sample, small pieces of membranes were cut from each batch and immersed into liquid nitrogen for a few minutes until the samples hardened. After removal from the liquid, the samples were broken, the fracture's surface was cleaned and coated with a gold layer to increase their conductivity. Fig. 4 shows the features of the microstructure's cross-section and porous structure of the fabricated PES and CNTs/PES membranes. The cross-sectional SEM micrographs of PES sample (Fig. (4A)) show that the

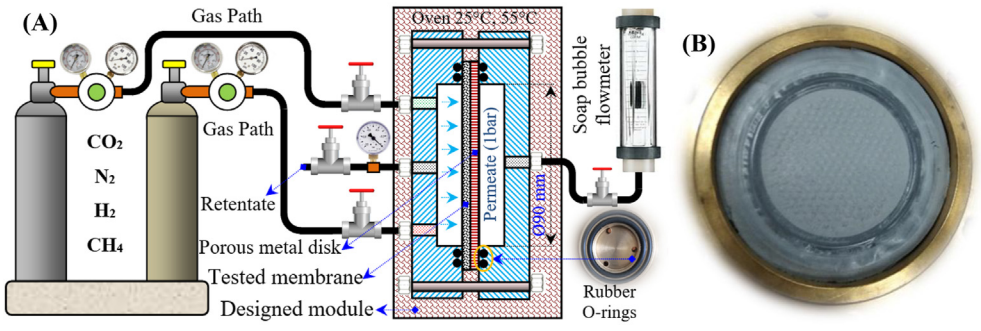

Fig. 3 – (A) Scheme of the set-up used in gas permeation measurements and (B) Image of the prepared CNTs/PES membranes after testing.

Table 1 – Parameters of gas permeability ($P_{i,j}$) and selectivity.

Parameters	Definition
P_i	Permeation coefficients of CO2
P_j	Permeation coefficients of N2 or H2 or CH4
$\alpha_{i/j}$	Ideal selectivity of CO2 and N2 or H2 or CH4
Q_i	Gas flux through the membrane
A	Effective area of the membrane
l	Membrane thickness
s	Solubility of CO2, N2, H2, and CH4
ΔP	Pressure change

membrane is composed of porous and dense layers formed during the solidification process, drying, and solvent evaporation as a result of fast solvent–non-solvent exchange in the interface of the casted films followed by generation of repulsive forces between the fabricated films and DI water, hence leading to immediate deposition of the PES molecules at the interface and creation of the dense layer [44]. It seems that the porous layer is characterized by big thickness and high strength, if compared with the dense layer. This porous layer was used during the separation process as a pre-filter stage to capture larger particles and agglomerates, while the thin layer acted as a main filtration layer for gas separation based on molecule sizes [45].

Although all membranes have almost the same features, including porous and dense layers and pores, these features changed a little by adding CNTs of different concentrations. For example, the porous layer in PES sample contained big pores with a size up to 50 μm, while the size of these pores began to increase significantly by adding CNTs to the matrix due to the expansion of the pores and their tendency to stick together as shown in the porous layer in Fig. (4B-D). The same features appeared in the pores in dense layers with some refining in the surface of pores Fig. (4A_1-D_1), where addition of CNTs to the matrix lad to restricted conformational freedom of PES chains and prevented the PES chains from joining together during the solidification process, which resulted in curvature on the surface at the microscale, followed by reduced crystallinity of the membrane and increase in amorphous and free volume fraction, which aided transportation of gases through the membranes [46,47]. In order to determine the size of these pores generated on dense layers and their porosity, the pore size distribution measurement was performed, as illustrated in the next section.

3.2. *Pore size distribution*

Since it was difficult to measure the pore size in the membranes manufactured with SEM precisely, the pore size distribution using a capillary flow porometer was measured. The measurements showed that PES membrane had bigger pores in the range of 84 ± 9 nm, while the measurements of PES membrane modified by CNTs revealed smaller pores located in the range of 50–70 nm depending on the concentration of CNTs in the prepared matrix, where the pores became very fine and smaller, especially at high loading of CNTs. These results agree with the results in literature [31,32]. Besides, the porosity of the neat membrane increased by adding 0.03 wt.% of CNTs from 81.7% to 88.4% and these results are confirmed by the membrane morphology. Having refined the pores by adding CNTs, the neat and modified membranes were classified as ultrafiltration membranes characterized by porosity (<0.1 μm) [48].

3.3. *Chemical composition of the synthesized CNTs/PES membranes*

The crystallinity of polymers is one of the key factors that has significant effect on gas transport properties through the membranes, where gas permeation through the membranes can happen in the amorphous stage or through the interstices between crystallites as a result of increased free space convenient for diffusion and the winding path around the crystallite [49]. XRD was used to examine the effect of CNTs addition on the crystallinity of membranes. Fig. (5A) shows XRD spectra of CNTs/PES membranes with different loadings of CNTs in the range of 0–0.03 wt.%. It is clear that

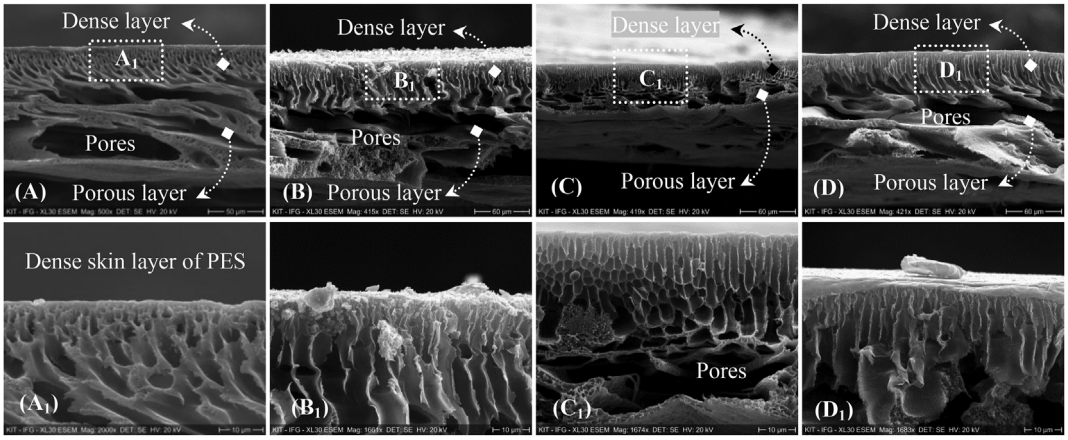

Fig. 4 – Cross-sectional SEM photos of (A) PES (B) CNTs/PES1 (C) CNTs/PES2 (D) CNTs/PES3 membranes.

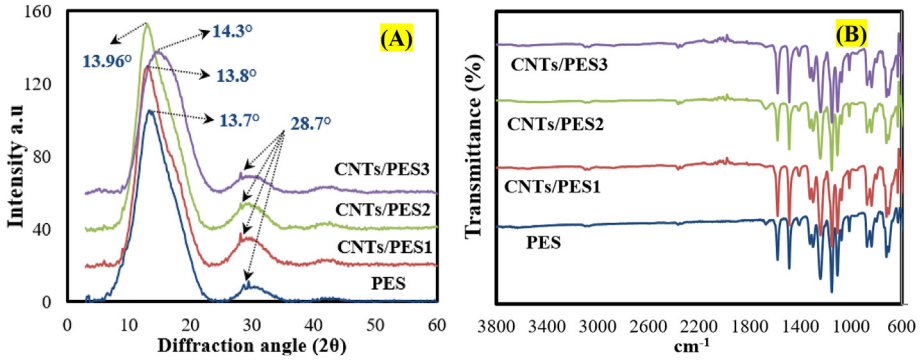

Fig. 5 – (A) XRD and (B) FTIR analysis of the fabricated CNTs/PES membranes.

the neat membrane sample (PES) is mainly amorphous with only sharp peak at around 2θ = 13.7° and these results agree with the results of pure polyethersulfone polymer [50]. After adding CNTs, it seems that no significant change in the sharp peak in XRD spectra was observed between the PES sample and the CNTs/PES samples, all of them having almost the same intensity. Although the amount of filler used in the research was very low and difficult to detect with XRD, a new reflection peak with very low intensity at 28.7° appeared and was assigned to CNTs phase of 0 0 2, 1 0 0 and 0 0 4 lattices, which means that addition of CNTs into PES subtract manifested a new amorphous structure. At higher CNTs concentrations (0.03 wt.%), the sharp peak at (13.7°) shifted slightly to higher angles with increasing CNTs load (14.3°), which confirmed the alteration of the average inter-segment spacing of PES chains and introduction of freer volume in the fabricated nanocomposite membranes [24], hence possible of increasing gas permeation performance through the membranes.

Fig. (5B) shows the FTIR spectra of the CNTs/PES nanocomposite membranes. As shown in the results, the FTIR spectrum of the tested membranes exhibited several broad absorbance peaks: at 558 cm^{-1} corresponding to SO2 scissors deformation, 1150 and 1170 cm^{-1} attributed to SO2 symmetric stretch, 1240 cm^{-1} corresponding to Aryl-O-aryl C–O stretch, 1300 and 1328 cm^{-1} attributed to SO2 asymmetric stretch, 1725 cm^{-1} and 1663 cm^{-1} corresponding to the carbonyl group (-C=O) in the lactic acid groups, 1570 cm^{-1} and 1482 cm^{-1} attributed to C=C skeleton in aromatic ring, and 1097 cm^{-1} attributed to –C–O stretching vibration of the lactic acid groups, and 3000–3200 cm^{-1} related to Aromatic CH stretches [42]. It seems that the FTIR spectra of CNTs/PES samples are similar to PES membrane FTIR results, with a new peak with low intensity appearing at 1995 cm^{-1} due to a carbonyl group produced by a double bonded carbon and oxygen (C=O), which corresponds to CNTs [24]. The presence of carbonyl group confirms that CNTs incorporated in the PES matrix has improved the free space region.

3.4. *Mechanical behaviour of the synthesized CNTs/PES membranes*

Fig. (6A-C) shows images of the prepared mechanical samples, stress–strain curves, and the measured mechanical data of the prepared CNTs/PES membranes samples, respectively. As shown in the stress–strain curves, PES sample had bigger strength (2.63 ± 0.18 MPa), strain (6.4 ± 0.27%), and elasticity modulus (200 ± 12.58 MPa) compared with nanocomposite samples. Having added CNTs to the PES matrix, all these parameters decreased significantly because of increase in the amorphous phase structure of PES and increased free volume of PES chains, as explained in XRD and FTIR results [44,51]. These free volume features in the form of pores (as shown in SEM photos Fig. (4)) acted as micro-cracks inside the CNTs/PES membranes, thus leading to decrease in the size of actual solid cross-section area of CNTs/PES membranes and merging

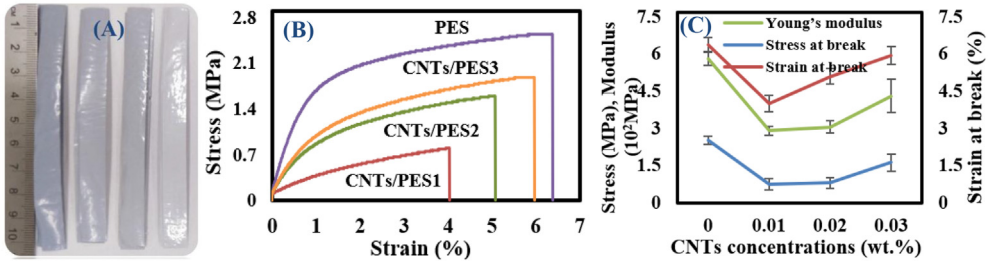

Fig. 6 – A) Images of mechanical samples, B) Stress–Strain curves and C) Stress–Strain values of the synthesized PES and CNTs/PES membranes.

together under the applied load, what could make it easier to destruct them under the applied load and reduce their mechanical performance.

3.5. *Thermal behaviour of the synthesized CNTs/PES membranes*

Fig. 7 displays TGA curves of CNTs/PES membranes and their decomposition phases in terms of weight loss in each decomposition stage. As shown in the figure, the TGA curves showed that PES and its nanocomposite can decompose in three stages in the temperature range from 25 to 900 °C with a total weight loss estimated at 57–65 wt.% (depending on the concentration of CNTs in the prepared matrix). The first stage is responsible for removal of moisture and solvent residue evaporation in the temperature range of 25–360 °C. It was evident that all the tested samples had almost the same features in this zone with very small weight loss (1.2 wt%). It was due to the successful preparation process of membranes by removing of all of these components during the drying process [42].

With regard to the second degradation stage (main decomposition zone), it was composed of two main decomposition components in all the tested samples. The first sector in this zone corresponded to the random-chain disengage mechanism of the basic PVP chain with weight loss in the range 8–11 wt.%, while the second sector referred to decomposition of PES in the range (456–610 °C) with weight loss estimated at 47–36 wt.% [52]. The final decomposition phase represented char and ash formation in the range (611–900 °C) at the end of reaction. It is clear that PES sample had lower thermal stability in terms of total weight loss (65 wt.%), while CNTs/PES membranes had higher thermal stability, especially at 0.02 wt.% of CNTs (55 wt.%) with improvement of 15%. These results agree with the results in the literature, which proves that nanofiller inorganic, including CNTs can be used to improve thermal stability of thin films [53,54].

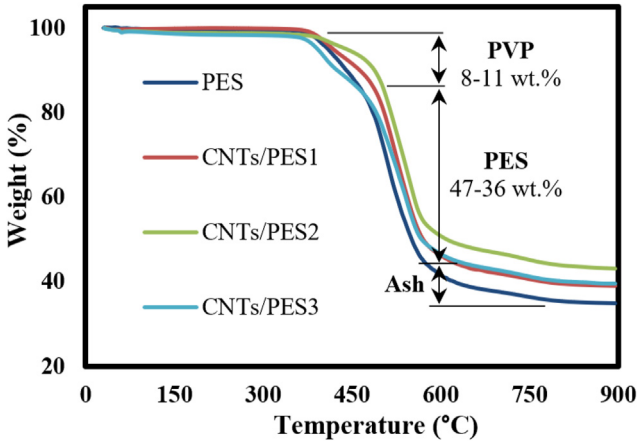

Fig. 7 – TGA analysis of the synthesized PES and CNTs/PES membranes.

3.6. *Evaluation of gas permeabilities*

Fig. (8A-D) shows the permeation measurements of CO2, N2, H2, and CH4 gases of the synthesized PES membrane and its nanocomposite (CNTs/PES1, CNTs/PES2, and CNTs/PES3) using a gas separation test rig under different feed pressures (1–6 bar) and different temperatures (20, 40, and 60 °C). For simplicity, in all figures and samples, solid, dotted, and dashed curves indicate the permeation measurements of CO2, N2, H2, and CH4 gases at 20 °C, 40 °C, and 60 °C, respectively. Also, and due to the significant difference in gas permeabilities of neat and nanocomposite membranes, the primary axes (left vertical axes) were allocated to the permeabilities of PES membrane, while the secondary axes (right vertical axes) were allocated to the permeabilities of CNTs/PES membranes.

Fig. (8A-D) shows H2, CH4, N2, CO2 permeabilities of PES and CNTs/PES membranes under the specified testing conditions. It is clear that gas permeabilities of PES membranes had the following tendency: N2 (10.5–15.4 Barrer) > CO2 (8.8–14.2 Barrer) > H2 (8.4–12.1 Barrer) > CH4 (3.4–5.6 Barrer) because of the difference in the size of the molecules of these gases in the range of 2.4–3.8 Å, where smaller gas molecules pass faster and freely through the pore channels, compared with larger gas molecules [55]. Also, the separation using these types of these polymeric membranes is governed by two main parameters, gas molecule size as listed before and polymer adsorption or capture of gases [56]. Besides the high ability of CNTs to absorb CO2 and some other gases, which leads to changing the permeability trends [57]. In addition, it seems that H2, CH4, N2, CO2 permeabilities increased gradually with increase of the applied pressure and temperature due to the plasticizing of the membranes and increase in their polymer matrix chain flexibility. Besides, the increase of temperature led to enhanced kinetic energies in the molecules of these gases, thus increasing their permeabilities [58]. However, some variation in gas permeabilities were observed with the change of temperature due to two main reasons; the first relates to plasticization effect in the tested PES under the applied temperature, while the second reason relates to the behaviour and characters of the tested gas that changes with the applied heat. Where the temperature of the gas is directly proportional to its pressure [59], which means that at 20 °C, the gas pressure in the membrane permeation module (Fig. (3)) is relatively low and increases at 40 and 60 °C. Where at the higher temperature the particles of gas in the module moving with a greater energy, what lead to more collisions randomly with each other and the sides of the testing module and hence the pressure is increased [60]. Therefore, obtained some variation in the results as a results of these randomly.

In case of CNTs/PES membranes, it was observed that CO_2, N_2, H_2, and CH_4 permeabilities had increased significantly with regard to all nanocomposite membranes, which means that addition of CNTs to PES matrix would enhance its permeability in general by increasing diffusivity even at low concentration of CNTs (0.01–0.03 wt.%). So, addition of CNTs leads to disrupting the PES chains and increase in the void volume of the membranes, thus producing more unbound places, which helps to transport gases easily through the PES chains [61]. Also, it was noted that the gas permeabilities

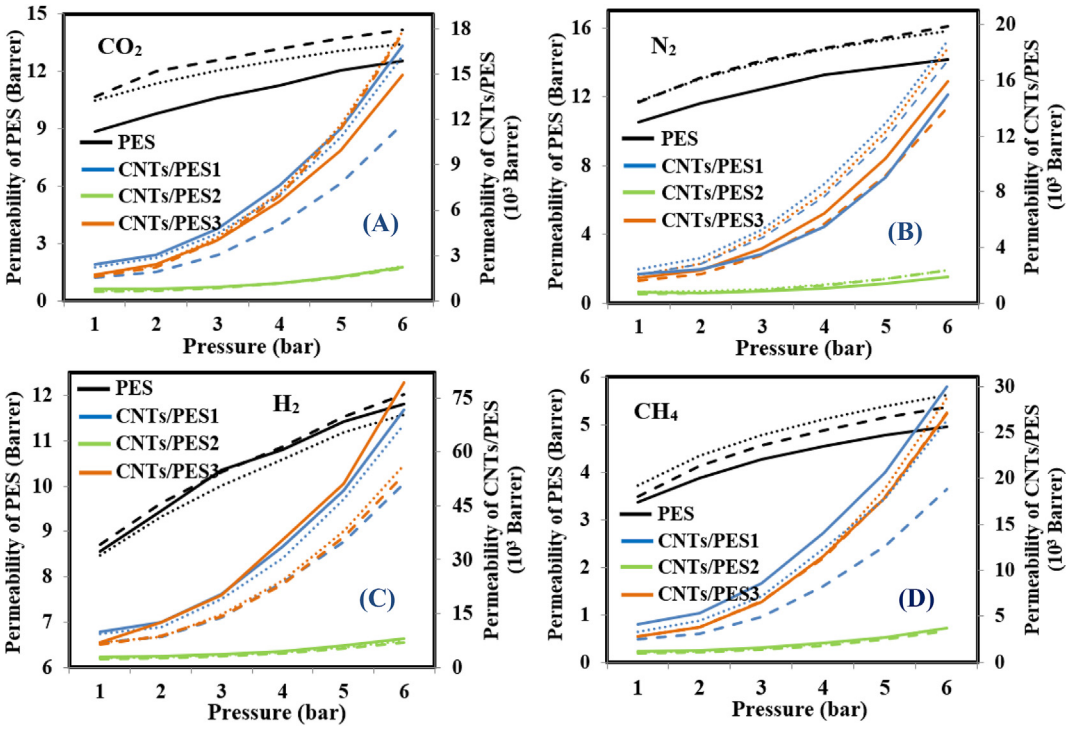

Fig. 8 – Effect of applied pressure and temperature on A-D) CO_2, N_2, H_2, and CH_4 permeabilities of the synthesized PES and CNTs/PES membranes, respectively.

increased gradually with increase in pressure and temperature, similarly to the neat membranes. However, in case of CNTs/PES2 sample, it was observed that the permeability of that sample was very low compared with CNTs/PES1 and CNTs/PES3 samples because of uniform distribution of CNTs in the sample, hence increasing the crystallinity degree of the matrix with partial alignment of their molecular chains and forming lamellae regions impeding transportation of gas through the membranes [62]. Meanwhile, the random distribution of CNTs in the prepared matrix led to decrease in crystallinity degree of CNTs/PES1 and CNTs/PES3 membranes followed by improvement in their porosity due to disruption of the PES chains, thus increasing gas permeabilities. Also, by adding CNTs to PES polymer, the matrix chain gained more flexibility, thus increasing the permeability significantly, especially at high temperature and pressure.

In order to facilitate the comparison process between the permeabilities of the neat and CNTs/PES membranes, the average (H2, CH4, N2, CO2) permeabilities of all measured values (at 1–6 bar and 20–60 °C) for each batch were calculated and used as a single value during the comparison process. All average H2, CH4, N2, CO2 permeabilities for PES and

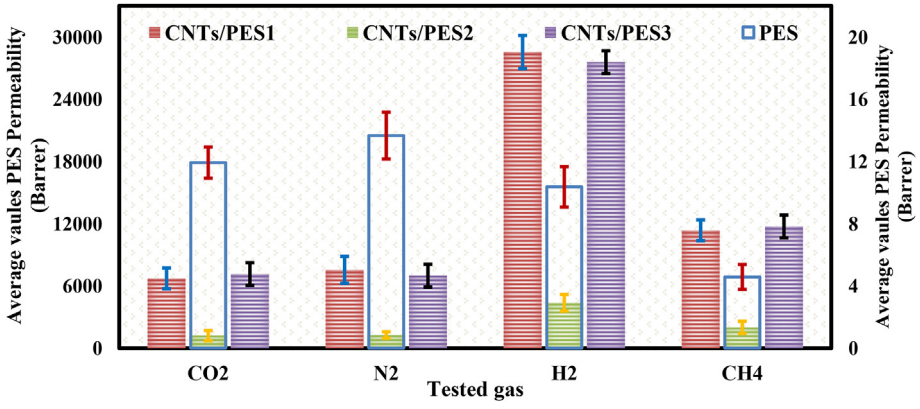

Fig. 9 – The average CO2, N2, H2, and CH4 permeability values of PES and CNTs/PES membranes.

CNTs/PES membranes are summarized in Fig. (9). According to Fig. (9), CNTs/PES1 and CNTs/PES3 membranes have the highest permeabilities of all gases with high values compared with the neat sample with the following tendency: H_2 (28,553 Barrer) > CH_4 (11,358 Barrer) > N_2 (7540 Barrer) > CO_2 (6720 Barrer) vs 10.4, 4.6, 13.7, and 12.3 Barrer, respectively in case of PES membranes. As shown, CNTs/PES membranes have ultra-permeabilities of H2, CH4, N2, CO2 gases compared with PES membranes. These results have a great potential when compared with those reported in the literature, which were used with high concentration of CNTs (0.5–10 wt.%) [33,34]; even PES membranes were enhanced by another types of fillers [15,63]. The result demonstrates that the CNTs/PES membranes with low concentration of CNTs exhibited high permeability.

3.7. Evaluation of gases selectivity

At present, polymer membranes are widely used in several fields, including carbon blocking, natural gas purification, biogas upgrading, etc. [22,42]. In order to determine the appropriate applications of the developed CNTs/PES membranes, the selectivity was calculated for all gases using Eq. (2), then identifying potential applications based on the obtained selectivity. Looking at researches and current challenges, two main applications were taken into account: a) CO2 separation for environmental applications and b) CH4/N2 and H2/N2 separation for clear energy applications. Based on that, this section was focused on these two topics. Also, this section was divided into two parts: the first part was focused on evaluation of CO2/N2, CO2/H2, and CO2/CH4 selectivity for carbon separation applications, while the second part was focused on evaluation of CH4/N2 and H2/N2 selectivity for clean energy applications.

3.7.1. CO2 separation applications

Fig. (10A-C) shows the effect of adding CNTs at tested temperatures (20, 40, and 60 °C) and pressures (1–6 bar) on the ideal CO2/CH4, CO2/N2, CO2/H2, and CO2/CH4 selectivity of the prepared PES and CNTs/PES membranes. In these figures, the primary axes were allocated to the selectivity of PES membrane, while the secondary axes were allocated to the selectivity of CNTs/PES membranes. It clear that CNTs/PES membranes have higher CO2/N2 ideal selectivity than neat sample with improvement of 29%. This is due to larger free spaces in CNTs/PES membranes acting as a strong CO2 adsorbent, hence helping the CO2 permeability over N2 gas in the tested membrane. This result is almost similar to the results obtained by Kamble et al. (2020), when PES was mixed with 2D materials and ionic liquid [15]. Also, the selectivity was increased with increase of the tested temperature and pressure. CNTs membranes manifested a very weak CO2/H2 and CO2/CH4 selectivity (0.3 and 0.4%) compared with PES membranes. All average selectivity values (for all measurement at 1–6 bar and 20–60 °C) of PES and CNTs/PES membranes are shown in Fig. (10D). Based on these results, CNTs/PES membranes with low CNTs content are recommended in case of CO2/N2 separation with ultra-permeability and high selectivity.

3.7.2. Clean energy applications

Fig. 11 shows the effect of adding of CNTs at tested temperatures (20–60 °C) and pressures (1–6 bar) on CH4/N2 and H2/N2 selectivity of the prepared PES membranes. It clear that the selectivity of CH4/N2 and H2/N2 of PES and CNTs/PES membranes proved a rapidly growing tendency up to 6 bars (PES) and 4 bars (CNTs/PES). However, PES membranes provided lower CH4/N2 and H2/N2 selectivity with average values of 0.33 and 0.76, respectively. As the content of CNTs increased up to 0.01 and 0.03 wt.%, CH4/N2 and H2/N2 selectivity was further increased up to 1.62 and 3.95. These significant results of CH4/N2 and H2/N2 selectivity were obtained due to the increased free volume and molecular space, enhanced CH4 and H2 permeabilities, and smaller kinetic diameters, H2 (0.24 Å) < N2 (0.36 Å) < CH4 (0.38 Å), thus resulting in higher diffusion [64]. Although N2 gas had smaller kinetic diameter than CH4, however, the results showed that N2 had smaller permeability and selectivity because of CH4 and H2 higher permeabilities, resulting in more forceful interactions of N2 with organic compounds [65]. Although this is the first research developed to study the CH4/N2 and H2/N2 selectivity of PES and their nanocomposite membranes, however, in literature, there may be encountered several types of membranes developed for that purpose by Yang et al. (2019), Yu et al. (2021), Yang et al. (2020), Yuan et al. (2021), Jiang et al. (2020), Azar et al. (2019), etc. [38,65–69], and the maximum CH4/N2 and H2/N2 selectivity was 2.3 (CH4/N2) and 4.3 (H2/N2). This means that PES membranes reinforced with low concentration of CNTs have better CH4/N2 and H2/N2 selectivity than the membranes listed above (twice as good). Therefore, the PES membranes incorporating low concentration of CNTs could be used as potential candidates to separate effectively CH4/N2 and H2/N2 for clean energy extraction applications.

3.7.3. Gas separation membrane mechanism

As shown in the results of selectivity in the section above, the developed CNTs/PES membranes have a high potential in separation of flammable gases (CH4 and H2) from CH4/N2 and H2/N2 mixture with high permeability, when compared with other gases. This section was developed to understand better the gas separation membrane mechanism of these gases using the CNTs/PES membranes. The separation mechanism was developed based on the result of pore size distribution, and cross-section and surface morphology of PES membrane and CNTs/PES1 membrane (optimum sample based on selectivity results), as illustrated in Fig. (12A-D). As shown in SEM images, the cross section of both membranes was composed of porous and dense layers containing pores of different sizes and shapes (Fig. (12A, B)). The pores of porous layer in CNTs/PES1 sample are characterized by their large size, steady shape and high porosity (88.4%), when compared with PES sample (81.7%). These big pores contribute a lot to blocking of gases with big particles size and agglomerates. On the contrary, the pores of dense skin layer in CNTs/PES1 sample are characterized by their fine size. They are smoother than PES due to surface modification caused by addition of CNTs. These pores are used in the main filtration process to separate gases based on molecule sizes of the gases. It is clear that a phase

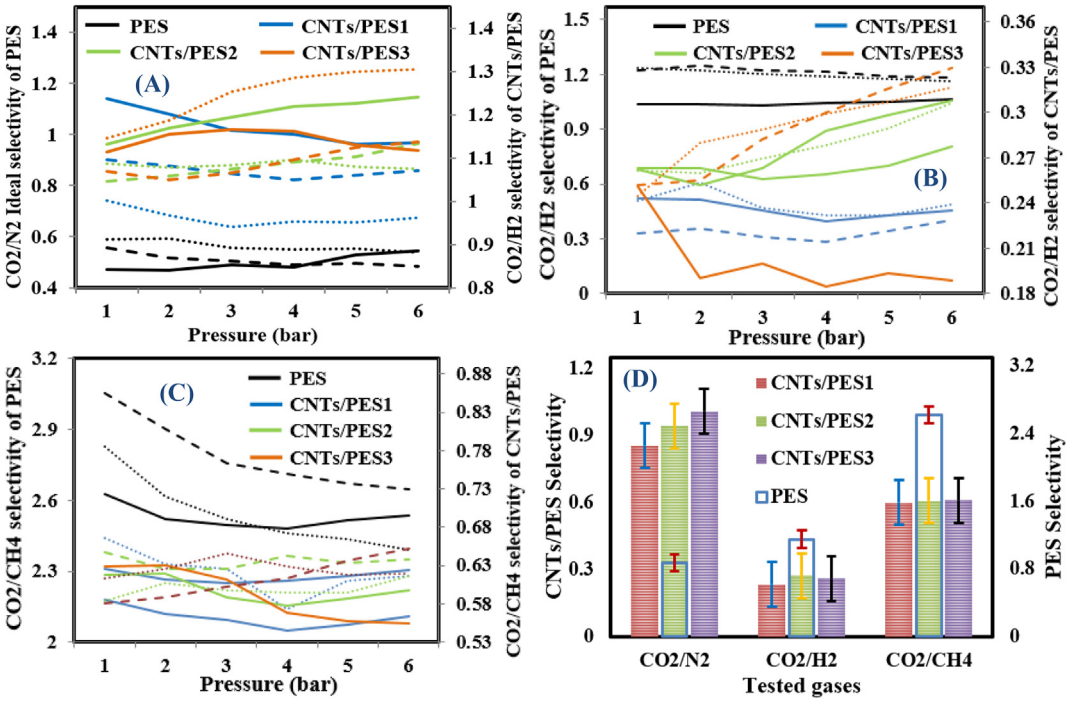

Fig. 10 – A-C) CO_2/N_2, CO_2/N_2, and CO_2/CH_4 selectivity of PES and CNTs/PES membranes at different temperatures (20–60 °C) and pressures (1–6 bar), and D) The average selectivity values of PES and CNTs/PES membranes.

inversion process which was used in the present research to prepare the membranes was applied successfully to fabricate the infinite number of membranes with uniform size and distribution on the surface, as shown in SEM surface morphology images Fig. (12C, D). Also, it is clear that the size of these pores decreased significantly by adding CNTs (from 80 to 50 nm), hence helping to block bigger gas particles.

In order to explain what happened to these pores after having mixed them with low-concentration CNTs, schematic drawings (Fig. (12E, F)) for the cross section of these pores (in dense layer) were made. As shown in the sketch (Fig. (12E)), the pores of PES membrane have a round shape containing throats (necks) in the middle that impede the movement of gases. Also, the internal surface looks curved and rough, thus resulting in bigger friction between the pores' surface and outer surfaces of transferred gases, hence decreasing the gas permeabilities [70]. All these defects in surface morphology can be addressed by adding a small amount of CNTs; then the surfaces of the pores become flatter and smoother allowing easier and faster gas transfer. It is worth mentioning that a high concentration of CNTs can clog the pores of membranes. In particular, CNTs have bigger length than diameter and it is hard to control their orientation in the matrix, thus resulting in shorter lifetime of membranes and big working costs [46].

Finally, with regard to separation mechanism of CH4/N2 and H2/N2, according to the data provided above, the

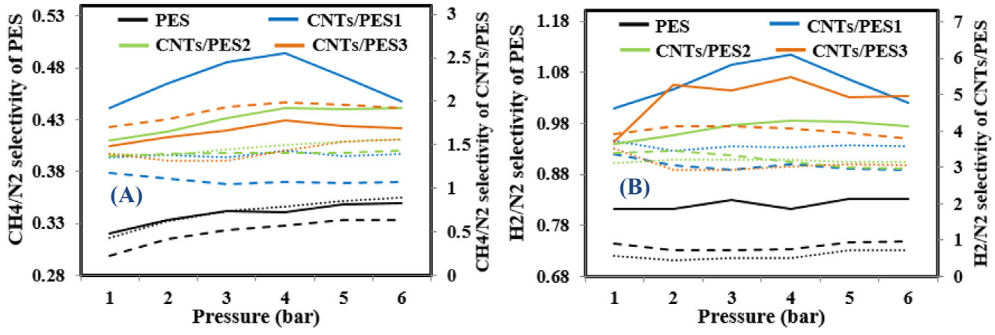

Fig. 11 – A) CH4/N2 selectivity and B) H2/N2 selectivity of PES and CNTs/PES membranes at different temperatures (20–60 °C) and pressures (1–6 bar).

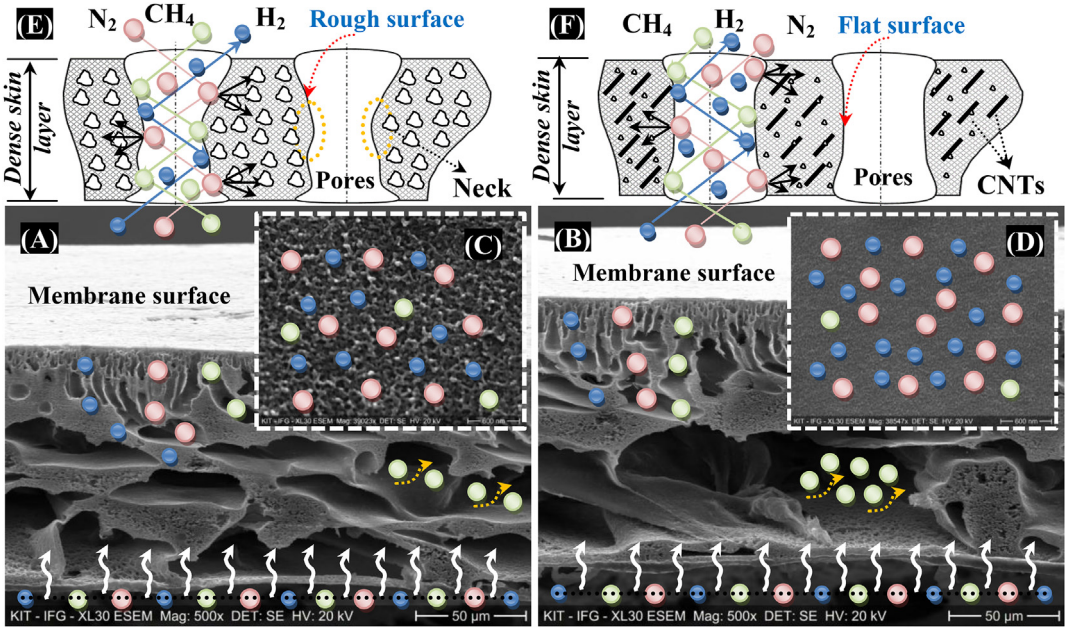

Fig. 12 – Mechanism for gas separation PES and CNTs/PES membranes.

fabricated membranes have pore sizes in the range of 50–84 nm, and this means that the separation mechanism conforms with Knudsen Diffusion principle that uses the inverse square root formula of the molecular weight [71]. According to this separation concept, the separation is achieved at the moment of gas–wall collisions, as shown in Fig. (12E, F). Since the surface area of wall of CNTs/PES membrane is much larger than that of PES membrane, the separation process was performed faster. Also, these bigger walls can absorb some of N2 particles and some of these particles can escape inside the pores encountered in the porous layer. N2 particles, especially have kinetic energy lower than H2, while CH4 can pass before these gases, as shown in Fig. (12E, F) [68], which leads to significant increase in H2 and CH4 permeability, when compared with N2 and their CH4/N2 and H2/N2 selectivity, as well.

4. Conclusions

In this research, carbon nanotubes (CNTs) with very low concentration (0.01–0.03 wt.%) were successfully embedded into Polysulfone (PES) for fabrication of ultra-permeable nanocomposite membranes (CNTs/PES) with high H2/N2 and CH4/N2 selectivity, using a doctor blade process. The microstructure and pore size distribution showed that CNTs/PES membranes contain a thin dense layer of fine pores (50 nm) and porous layers made of pores with high porosity. The chemical analysis using XRD and FTIR revealed uniform incorporation of CNTs in the prepared matrix and decreased crystallinity of PES leading to formation of more free spaces, thus helping to transfer gasthrough CNTs/PES membranes. Also, the thermal analysis showed that CNTs/PES membranes have thermal stability similar to that of a neat membrane. Regarding the permeability measurements, the CNTs/PES membranes showed the ability to operate in warm ambient and under high pressure with excellent permeability with the following tendency: $H_2 > CH_4 > N_2 > CO_2$. Also, CNTs/PES membranes with 0.01 wt.% of CNTs proved good CO2/N2 selectivity (1.2), when compared with PES sample (0.87). In addition, CNTs/PES membranes manifested excellent CH4/N2 and H2/N2 selectivity estimated at 1.62 and 3.95 vs 0.33 and 0.76 for the neat membranes. Based on that, the PES membranes reinforced by low concentration of CNTs (0.01–0.03 wt.%) can be classified as a promising technology for separation of flammable gases (CH4 and H2) from CH4/N2 and H2/N2 mixture with ultra-permeability.

Declaration of Competing Interest

The authors declare that they have no known competing financial interests or personal relationships that could have appeared to influence the work reported in this paper.

Acknowledgement

This project has received funding from the Research Council of Lithuania (LMTLT), agreement No. [S-MIP-20-27].

REFERENCES

[1] Yusuf A, Sodiq A, Giwa A, Eke J, Pikuda O, De Luca G, et al. A review of emerging trends in membrane science and technology for sustainable water treatment. J Clean Prod 2020. https://doi.org/10.1016/j.jclepro.2020.121867.

[2] Su R, Li S, Wu W, Song C, Liu G, Yu Y. Recent progress in electrospun nanofibrous membranes for oil/water separation. Separation and Purification Technology; 2021. https://doi.org/10.1016/j.seppur.2020.117790.
[3] Di Domenico Ziero H, Buller LS, Mudhoo A, Ampese LC, Mussatto SI, Carneiro TF. An overview of subcritical and supercritical water treatment of different biomasses for protein and amino acids production and recovery. Journal of Environmental Chemical Engineering 2020. https://doi.org/10.1016/j.jece.2020.104406.
[4] Ang EYM, Toh W, Yeo J, Lin R, Liu Z, Geethalakshmi KR, et al. A review on low dimensional carbon desalination and gas separation membrane designs. J Membr Sci 2020. https://doi.org/10.1016/j.memsci.2019.117785.
[5] Elsaidi SK, Venna S, Sekizkardes AK, Steckel JA, Mohamed MH, Baker J, et al. Custom formulation of multicomponent mixed-matrix membranes for efficient post-combustion carbon capture. Cell Reports Physical Science 2020. https://doi.org/10.1016/j.xcrp.2020.100113.
[6] Bozorg M, Ramírez-Santos ÁA, Addis B, Piccialli V, Castel C, Favre E. Optimal process design of biogas upgrading membrane systems: polymeric vs high performance inorganic membrane materials. Chem Eng Sci 2020. https://doi.org/10.1016/j.ces.2020.115769.
[7] Nemestóthy N, Bélafi-Bakó K, Bakonyi P. Enhancement of dark fermentative H2 production by gas separation membranes: a review. In: Bioresource technology; 2020. https://doi.org/10.1016/j.biortech.2020.122828.
[8] Amirkhani F, Mosadegh M, Asghari M, Parnian MJ. The beneficial impacts of functional groups of CNT on structure and gas separation properties of PEBA mixed matrix membranes. Polym Test 2020. https://doi.org/10.1016/j.polymertesting.2019.106285.
[9] El-Sayed R, Osman TA, Toprak MS, Muhammed M, Uheida A. Composite nanofibers for highly efficient photocatalytic degradation of organic dyes from contaminated water. Environ Res 2016;145:18–25.
[10] Osman TA, Toprak MS, Muhammed M, Yilmaz Eda, Uheida A. Visible light photocatalytic reduction of Cr(VI) by surface modified CNT/Titanium dioxide composites nanofibers. J Mol Catal Chem 2016;424:45–53.
[11] Farnam M, Mukhtar H, Shariff A. Analysis of the influence of CMS variable percentages on pure PES membrane gas separation performance. Procedia Engineering; 2016. https://doi.org/10.1016/j.proeng.2016.06.449.
[12] Pang R, Chen KK, Han Y, Ho WSW. Highly permeable polyethersulfone substrates with bicontinuous structure for composite membranes in CO2/N2 separation. J Membr Sci 2020. https://doi.org/10.1016/j.memsci.2020.118443.
[13] Notario B, Pinto J, Solorzano E, De Saja JA, Dumon M, Rodríguez-Pérez MA. Experimental validation of the Knudsen effect in nanocellular polymeric foams. Polymer 2015. https://doi.org/10.1016/j.polymer.2014.10.006.
[14] Farrokhara M, Dorosti F. New high permeable polysulfone/ionic liquid membrane for gas separation. Chin J Chem Eng 2020. https://doi.org/10.1016/j.cjche.2020.04.002.
[15] Kamble AR, Patel CM, Murthy ZVP. Polyethersulfone based MMMs with 2D materials and ionic liquid for CO2, N2 and CH4 separation. J Environ Manag 2020. https://doi.org/10.1016/j.jenvman.2020.110256.
[16] Yousef S, Eimontas J, Striūgas N, Trofimov E, Hamdy M, Abdelnaby MA. Conversion of end-of-life cotton banknotes into liquid fuel using mini-pyrolysis plant. J Clean Prod 2020. https://doi.org/10.1016/j.jclepro.2020.121612.
[17] Yousef S, Eimontas J, Striūgas N, Tatariants M, Abdelnaby MA, Tuckute S, et al. A sustainable bioenergy conversion strategy for textile waste with self-catalysts using mini-pyrolysis plant. Energy Conversion and Management; 2019. https://doi.org/10.1016/j.enconman.2019.06.050.
[18] Gustafsson M, Anderberg S. Dimensions and characteristics of biogas policies – modelling the European policy landscape. In: Renewable and sustainable energy reviews; 2021. https://doi.org/10.1016/j.rser.2020.110200.
[19] Niskanen J, Magnusson D. Understanding upscaling and stagnation of farm-based biogas production in Sweden through transitional and farming logics. J Clean Prod 2021. https://doi.org/10.1016/j.jclepro.2020.123235.
[20] Serbanescu OS, Voicu SI, Thakur VK. Polysulfone functionalized membranes: properties and challenges. In: Materials today chemistry; 2020. https://doi.org/10.1016/j.mtchem.2020.100302.
[21] Khalid A, Ibrahim A, Al-Hamouz OCS, Laoui T, Benamor A, Atieh MA. Fabrication of polysulfone nanocomposite membranes with silver-doped carbon nanotubes and their antifouling performance. J Appl Polym Sci 2017. https://doi.org/10.1002/app.44688.
[22] Sainath K, Modi A, Bellare J. In-situ growth of zeolitic imidazolate framework-67 nanoparticles on polysulfone/graphene oxide hollow fiber membranes enhance CO2/CH4 separation. J Membr Sci 2020. https://doi.org/10.1016/j.memsci.2020.118506.
[23] Mohamed Alaa, Nasser WS, Osman TA, Toprak MS, Muhammed M, Uheida A. Removal of chromium (VI) from aqueous solutions using surface modified composite nanofibers. J Colloid Interface Sci 2017;505:682–91.
[24] Wang L, Song X, Wang T, Wang S, Wang Z, Gao C. Fabrication and characterization of polyethersulfone/carbon nanotubes (PES/CNTs) based mixed matrix membranes (MMMs) for nanofiltration application. Appl Surf Sci 2015. https://doi.org/10.1016/j.apsusc.2014.12.183.
[25] Swain SS, Unnikrishnan L, Mohanty S, Nayak SK. Carbon nanotubes as potential candidate for separation of H2[sbnd]CO2 gas pairs. Int J Hydrogen Energy 2017. https://doi.org/10.1016/j.ijhydene.2017.09.152.
[26] Dube ST, Moutloali RM, Malinga SP. Hyperbranched polyethyleneimine/multi-walled carbon nanotubes polyethersulfone membrane incorporated with Fe-Cu bimetallic nanoparticles for water treatment. Journal of Environmental Chemical Engineering 2020. https://doi.org/10.1016/j.jece.2020.103962.
[27] Daramola MO, Hlanyane P, Sadare OO, Oluwasina OO, Iyuke SE. Performance of carbon nanotube/polysulfone (CNT/Psf) composite membranes during Oil–water mixture separation: effect of CNT dispersion method. Membranes 2017. https://doi.org/10.3390/membranes7010014.
[28] Mohamed Alaa, Yousef Samy, Abdelnaby Mohammed Ali, Osman TA, Hamawandi B, Toprak MS, et al. Photocatalytic degradation of organic dyes and enhanced mechanical properties of PAN/CNTs composite nanofibers. Separ Purif Technol 2017;182:219–23.
[29] Nikita K, Karkare P, Ray D, Aswal VK, Singh PS, Murthy CN. Understanding the morphology of MWCNT/PES mixed-matrix membranes using SANS: interpretation and rejection performance. Applied Water Science 2019. https://doi.org/10.1007/s13201-019-1035-4.
[30] Abidin MNZ, Goh PS, Ismail AF, Othman MHD, Hasbullah H, Said N, et al. Development of biocompatible and safe polyethersulfone hemodialysis membrane incorporated with functionalized multi-walled carbon nanotubes. Mater Sci Eng C 2017. https://doi.org/10.1016/j.msec.2017.03.273.
[31] Mangukiya S, Prajapati S, Kumar S, Aswal VK, Murthy CN. Polysulfone-based composite membranes with functionalized carbon nanotubes show controlled porosity and enhanced electrical conductivity. J Appl Polym Sci 2016. https://doi.org/10.1002/app.43778.

[32] Costa JB, Lima MJ, Sampaio MJ, Neves MC, Faria JL, Morales-Torres S, et al. Enhanced biocatalytic sustainability of laccase by immobilization on functionalized carbon nanotubes/polysulfone membranes. Chem Eng J 2019. https://doi.org/10.1016/j.cej.2018.08.178.
[33] Yazdi MG, Ivanic M, Mohamed Alaa, Uheida A. Surface modified composite nanofibers for the removal of indigo carmine dye from polluted water. RSC Adv 2018;8:24588–98.
[34] Ismail AF, Rahim NH, Mustafa A, Matsuura T, Ng BC, Abdullah S, et al. Gas separation performance of polyethersulfone/multi-walled carbon nanotubes mixed matrix membranes. Separation and Purification Technology; 2011. https://doi.org/10.1016/j.seppur.2011.03.031.
[35] Gumbi NN, Hu M, Mamba BB, Li J, Nxumalo EN. Macrovoid-free PES/SPSf/O-MWCNT ultrafiltration membranes with improved mechanical strength, antifouling and antibacterial properties. J Membr Sci 2018. https://doi.org/10.1016/j.memsci.2018.09.009.
[36] Liu C, Wang W, Zhu L, Cui F, Xie C, Chen X, et al. High-performance nanofiltration membrane with structurally controlled PES substrate containing electrically aligned CNTs. J Membr Sci 2020. https://doi.org/10.1016/j.memsci.2020.118104.
[37] Parsamanesh M, Mansourpanah Y, Dadkhah Tehrani A. Improving the efficacy of PES-based mixed matrix membranes incorporated with citric acid–amylose-modified MWCNTs for HA removal from water. Polym Bull 2020. https://doi.org/10.1007/s00289-020-03162-y.
[38] Jiang J, Islam S, Dong Q, Zhou F, Li S, Yu M. Deposition of an ultrathin palladium (Pd) coating on SAPO-34 membranes for enhanced H2/N2 separation. Int J Hydrogen Energy 2020. https://doi.org/10.1016/j.ijhydene.2020.09.087.
[39] Ren X, Sun T, Hu J, Wang S. Highly enhanced selectivity for the separation of CH4 over N2 on two ultra-microporous frameworks with multiple coordination modes. Microporous and Mesoporous Materials; 2014. https://doi.org/10.1016/j.micromeso.2013.11.038.
[40] Yousef S, Mohamed A. Mass production of CNTs using CVD multi-quartz tubes. J Mech Sci Technol 2016. https://doi.org/10.1007/s12206-016-1031-7.
[41] Mohamed A, Yousef S, Nasser WS, Osman TA, Knebel A, Sánchez EPV, et al. Rapid photocatalytic degradation of phenol from water using composite nanofibers under UV. Environ Sci Eur 2020. https://doi.org/10.1186/s12302-020-00436-0.
[42] Yousef S, Šereika J, Tonkonogovas A, Hashem T, Mohamed A. CO2/CH4, CO2/N2 and CO2/H2 selectivity performance of PES membranes under high pressure and temperature for biogas upgrading systems. Environmental Technology and Innovation 2021. https://doi.org/10.1016/j.eti.2020.101339.
[43] Yousef S, Sarwar Z, Šereika J, Striugas N, Krugly E, Danilovas PP, et al. A new industrial technology for mass production of graphene/peba membranes for CO2/CH4 selectivity with high dispersion, thermal and mechanical performance. Polymers 2020. https://doi.org/10.3390/POLYM12040831.
[44] Jiang Y, Zeng Q, Biswas P, Fortner JD. Graphene oxides as nanofillers in polysulfone ultrafiltration membranes: shape matters. J Membr Sci 2019. https://doi.org/10.1016/j.memsci.2019.03.056.
[45] Luque-Alled JM, Abdel-Karim A, Alberto M, Leaper S, Perez-Page M, Huang K, et al. Polyethersulfone membranes: from ultrafiltration to nanofiltration via the incorporation of APTS functionalized-graphene oxide. Separ Purif Technol 2020. https://doi.org/10.1016/j.seppur.2019.115836.
[46] Wang W, Zhu L, Shan B, Xie C, Liu C, Cui F, et al. Preparation and characterization of SLS-CNT/PES ultrafiltration membrane with antifouling and antibacterial properties. J Membr Sci 2018. https://doi.org/10.1016/j.memsci.2017.11.046.
[47] Kim S, Chen L, Johnson JK, Marand E. Polysulfone and functionalized carbon nanotube mixed matrix membranes for gas separation: theory and experiment. J Membr Sci 2007. https://doi.org/10.1016/j.memsci.2007.02.028.
[48] Liu S, Chu Y, Tang C, He S, Wu C. High-performance chlorinated polyvinyl chloride ultrafiltration membranes prepared by compound additives regulated non-solvent induced phase separation. J Membr Sci 2020. https://doi.org/10.1016/j.memsci.2020.118434.
[49] Markova SY, Gries T, Teplyakov VV. Poly(4-methyl-1-pentene) as a semicrystalline polymeric matrix for gas separating membranes. J Membr Sci 2020. https://doi.org/10.1016/j.memsci.2019.117754.
[50] Subadra SP, Yousef S, Griskevicius P, Makarevicius V. High-performance fiberglass/epoxy reinforced by functionalized CNTs for vehicle applications with less fuel consumption and greenhouse gas emissions. Polym Test 2020. https://doi.org/10.1016/j.polymertesting.2020.106480.
[51] Elele E, Shen Y, Tang J, Lei Q, Khusid B, Tkacik G, et al. Mechanical properties of polymeric microfiltration membranes. J Membr Sci 2019. https://doi.org/10.1016/j.memsci.2019.117351.
[52] Karim ShroukA, Mohamed Alaa, Abdel-Mottaleb MM, Osman TA, Khattab A. Mechanical properties and the characterization of polyacrylonitrile/carbon nanotube composite nanofiber. Arabian J Sci Eng 2018;43(9):4697–702.
[53] Shah P, Murthy CN. Studies on the porosity control of MWCNT/polysulfone composite membrane and its effect on metal removal. J Membr Sci 2013. https://doi.org/10.1016/j.memsci.2013.02.042.
[54] Sotto A, Boromand A, Balta S, Kim J, Van Der Bruggen B. Doping of polyethersulfone nanofiltration membranes: antifouling effect observed at ultralow concentrations of TiO2 nanoparticles. J Mater Chem 2011. https://doi.org/10.1039/c1jm11040c.
[55] Saqib S, Rafiq S, Muhammad N, Khan AL, Mukhtar A, Ullah S, et al. Sustainable mixed matrix membranes containing porphyrin and polysulfone Polymer for acid gas separations. J Hazard Mater 2021. https://doi.org/10.1016/j.jhazmat.2021.125155.
[56] Magi Meconi Giulia, Tomovska Radmila, Ronen Zangi. Adsorption of CO2 gas on graphene–polymer composites. Journal of CO2 Utilization 2019. https://doi.org/10.1016/j.jcou.2019.03.005.
[57] Liu L, Nicholson D, Bhatia SK. Adsorption of CH4 and CH4/CO2 mixtures in carbon nanotubes and disordered carbons: a molecular simulation study. Chem Eng Sci 2015. https://doi.org/10.1016/j.ces.2014.07.041.
[58] Alkhouzaam A, Khraisheh M, Atilhan M, Al-Muhtaseb SA, Qi L, Rooney D. High-pressure CO2/N2 and CO2/CH4 separation using dense polysulfone-supported ionic liquid membranes. J Nat Gas Sci Eng 2016;36:472–85.
[59] Liu L, Yang M, Zhang X, Mao J, Chai P. LNMR experimental study on the influence of gas pressure on methane adsorption law of middle-rank coal. J Nat Gas Sci Eng 2021. https://doi.org/10.1016/j.jngse.2021.103949.
[60] Yu S, Fang F, Tang L, Zhong X, Ding W. Study of particle transport and gas amplification mechanism in proportional counters. Appl Radiat Isot 2021. https://doi.org/10.1016/j.apradiso.2021.109591.
[61] Wong KC, Goh PS, Taniguchi T, Ismail AF, Zahri K. The role of geometrically different carbon-based fillers on the formation and gas separation performance of nanocomposite membrane. Carbon 2019. https://doi.org/10.1016/j.carbon.2019.04.031.
[62] Rayekan Iranagh F, Asghari M, Parnian MJ. Dispersion engineering of MWCNT to control structural and gas

transport properties of PU mixed matrix membranes. Journal of Environmental Chemical Engineering 2020. https://doi.org/10.1016/j.jece.2020.104493.

[63] Natarajan P, Sasikumar B, Elakkiya S, Arthanareeswaran G, Ismail AF, Youravong W, et al. Pillared cloisite 15A as an enhancement filler in polysulfone mixed matrix membranes for CO2/N2 and O2/N2 gas separation. J Nat Gas Sci Eng 2021. https://doi.org/10.1016/j.jngse.2020.103720.

[64] Huang X, Yao H, Cheng Z. Hydrogen separation membranes of polymeric materials nanostructured materials for next-generation energy storage and conversion. Springer Berlin Heidelberg; 2017. p. 85–116.

[65] Yang X, Zheng Y, Wang L, Guo Q, Shan H, Xu Z, et al. Application of CH4/N2 separation based on poly(styrene-b-isoprene-b-styrene)(SIS)-poly(dimethylsiloxane-co-methylhydrosiloxane)(PDMS-co-PMHS)crosslinked membrane. Reactive and functional polymers. 2019. https://doi.org/10.1016/j.reactfunctpolym.2019.05.014.

[66] Yu HJ, Shin JH, Lee AS, Hwang SS, Kim JH, Back S, et al. Tailoring selective pores of carbon molecular sieve membranes towards enhanced N2/CH4 separation efficiency. J Membr Sci 2020. https://doi.org/10.1016/j.memsci.2020.118814.

[67] Yang J, Bai H, Shang H, Wang J, Li J, Deng S. Experimental and simulation study on efficient CH4/N2 separation by pressure swing adsorption on silicalite-1 pellets. Chem Eng J 2020. https://doi.org/10.1016/j.cej.2020.124222.

[68] Azam Aydani, Brunetti Adele, Maghsoudi Hafez, Barbieri Giuseppe. CO2 separation from binary mixtures of CH4, N2, and H2 by using SSZ-13 zeolite membrane. Separ Purif Technol 2021:117796. https://doi.org/10.1016/j.seppur.2020.117796.

[69] Azar Ayda Nemati Vesali, Velioğlu Sadiye, Keskin Seda. Large-scale computational screening of metal organic framework (MOF) membranes and MOF-based polymer membranes for H2/N2 separations. ACS Sustainable Chem Eng 2019;7:9525–36.

[70] Mocanu A, Rusen E, Diacon A, Isopencu G, Mustăţea G, Şomoghi R, et al. Antimicrobial properties of polysulfone membranes modified with carbon nanofibers and silver nanoparticles. Mater Chem Phys 2019. https://doi.org/10.1016/j.matchemphys.2018.10.002.

[71] Shen W, Song F, Hu X, Zhu G, Zhu W. Experimental study on flow characteristics of gas transport in micro- and nanoscale pores. Sci Rep 2019. https://doi.org/10.1038/s41598-019-46430-2.